

UC Berkeley

Development and Technology

Title

Modeling the Flow in an Underflow Plenum

Permalink

<https://escholarship.org/uc/item/2t64d9gc>

Authors

Linden, P F
Yu, J. K.

Publication Date

2007-04-04



Energy Development and Technology 010

**“Modeling the Flow in an
Underflow Plenum”**

P.F.Linden & J.K.Yu

April 2007

Contact Info.: Phone:1-858-822-2274; Fax:1-858-534-7720;
E-Mail: Plinden@ucsd.edu

This paper is part of the University of California Energy Institute's (UCEI) Energy Development and Technology Working Paper Series. UCEI is a multi-campus research unit of the University of California located on the Berkeley campus.

UC Energy Institute
2547 Channing Way
Berkeley, California 94720-5180
www.ucei.org

This report was issued in order to disseminate results of and information about energy research at the University of California campuses. Any conclusions or opinions expressed are those of the authors and not necessarily those of the Regents of the University of California, the University of California Energy Institute or the sponsors of the research. Readers with further interest in or questions about the subject matter of the report are encouraged to contact the authors directly.



Modeling the flow in an underflow plenum

Final Report

P.F.Linden* & J.K.Yu

* Contact Info.: Phone:1-858-822-2274; Fax:1-858-534-7720; E-Mail:
pflinden@ucsd.edu

1 Introduction

The object of this research is to examine the flow in a plenum of an underfloor air distribution system (UFAD). UFAD installations have often performed poorly because the air entering the space through different vents attached to the plenum has different temperatures. The temperature differences vary in time and can be as much as 5 °C from diffuser to diffuser. It is believed that these temperature inhomogeneities are a result of circulating patterns established in the air flow in the plenum, and that these circulations, in turn, are a result of specific supply and plenum geometries.

We have carried out laboratory simulations and numerical modeling of the plenum flow in an attempt to establish the dependence of the flow patterns on the supply configurations. We have conducted a systematic study of the flow patterns for different forcing arrangements and discuss the implications for plenum design. In each case the plenum is square in plan form and the configurations studied are:

- One source jet in the middle of a side wall
- Two source jets in the same side wall with the same direction
- Two source jets in opposite side walls with opposite directions
- Four source jets in four side walls to generate an initial torque

For the first configuration, we investigate laminar and turbulent jet behavior for two the aspect ratios of the horizontal and vertical length scales in order to assess the two-dimensionality of the flow. For the two co-flowing and counterflowing arrangements we investigate the effects of coalescence of the jets.

In the multiple jet cases the interactions of the jets established strong and, in many cases, persistent circulations. These flows were studied in the laboratory using Particle Image Velocimetry (PIV). A RNG K- ϵ turbulent closure was used for numerical calculations. The numerical calculations also allowed the thermal performance to be evaluated by the addition of heat transfer into the plenum from the top and bottom boundaries.

2 Experimental and Numerical Methods

2.1 Experiments

Experiments were performed in a square-section tank of inner dimensions $59.7 \times 59.7 \times 45$ cm and a plexiglass plate partition supported by vertical columns was placed inside the tanks

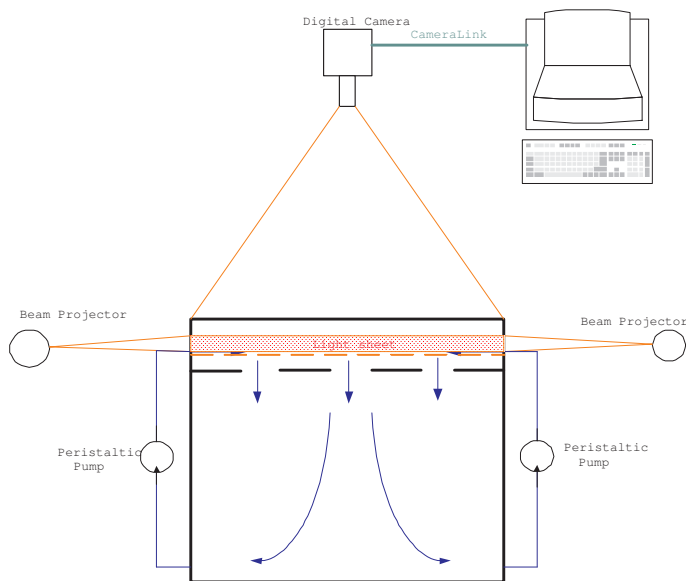


Figure 1: The schematic diagram of the experimental apparatus.

to separate the plenum from the space below. The height of lower space was fixed at 19 cm. The lower chamber used for even distribution of pressure across the holes which represent the room in a UFAD system. The free surface between the water and air is assumed to be a vertical symmetry plane. Thus the slip boundary in the experiment can be assumed to show the same flow pattern of two no-slip boundaries of a double depth plenum. This configuration for the plenum provides a clear image of particles and convenient set up of the camera.(Fig. 1)

A horizontal light sheet was used to illuminate seeded PIV particles on a horizontal layer. A peristaltic pump circulated water from sinks placed on the bottom and source jets in the plenum (Fig.1). The Reynolds number $Re = Vd/\nu$ was calculated from the temporal mean volume flow rate, d is the inner diameter of the sources and ν is the kinematic viscosity of the fluid. Re was approximately $O(10^2)$, so source jets are laminar (Fig. 2).

2.2 Numerical Method

The Reynolds Averaged Numerical Simulation (RANS) model was used for three dimensional thermal simulation of the flow with $Re O(10^5)$. A RNG (ReNormalized Group) K- ϵ scheme was employed for turbulent modeling, which is widely used for subsonic flow simulation due to low generation of excessive turbulent viscosity(Choudary1993). The computation

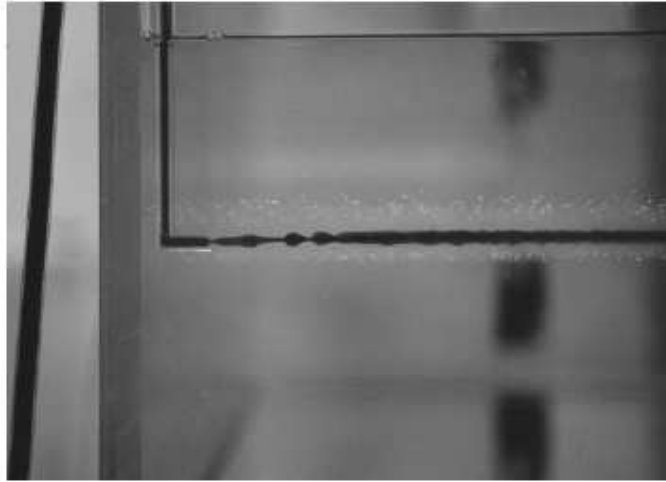


Figure 2: Dyed image of source flow (KL 2002).

was performed by FLUENT 6.2.22. The RNG the turbulence model is derived from the Navier-Stokes equations by a mathematical technique called “renormalization group” method (Fluent Inc.).

Eight IBM 2528 Power4+ CPUs provided by DATASTAR computing server on San Diego Supercomputer Center (SDSC) was used for three dimensional double-precision computation. The second order implicit scheme is used for time marching and PISO scheme is used for pressure-velocity coupling. The spatial derivatives are computed using QUICK scheme which is based on a weighted average of second-order-upwind and central interpolations of the variable (Leonard 1990).

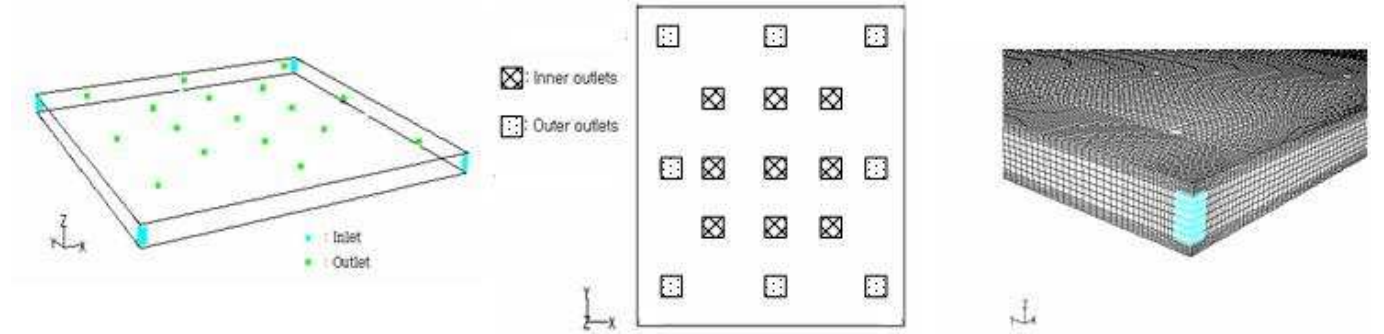


Figure 3: Computation mesh and inlet and outlet boundary position.

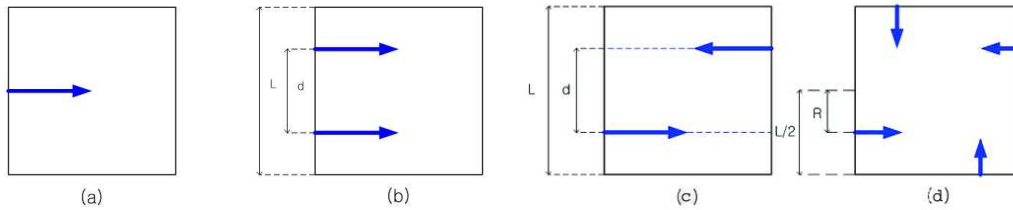


Figure 4: Horizontal view of source jet : (a) One source; (b) Two sources with same direction; (c) Two sources with opposite directions; (d) Four sources.

3 Results

3.1 Flow patterns of each configuration

The plan view of the horizontal velocity field was measured and compared to the numerical simulations (Fig. 5), with generally good qualitative agreement. In the one-source configuration, a dipole vortex pair induced by impingement of the jet on the far wall divided the flow into three regions: a strong entrainment region, a dipole vortex region, and an impingement region (Fig. 6).

The distance between the two source jets is an important parameter (Fig. 7). When $d/L > 0.33$, the merged jets are separated by an inward recirculating vortex and the vortex grows in size as d/L increases. Two source jets in opposite directions show totally different

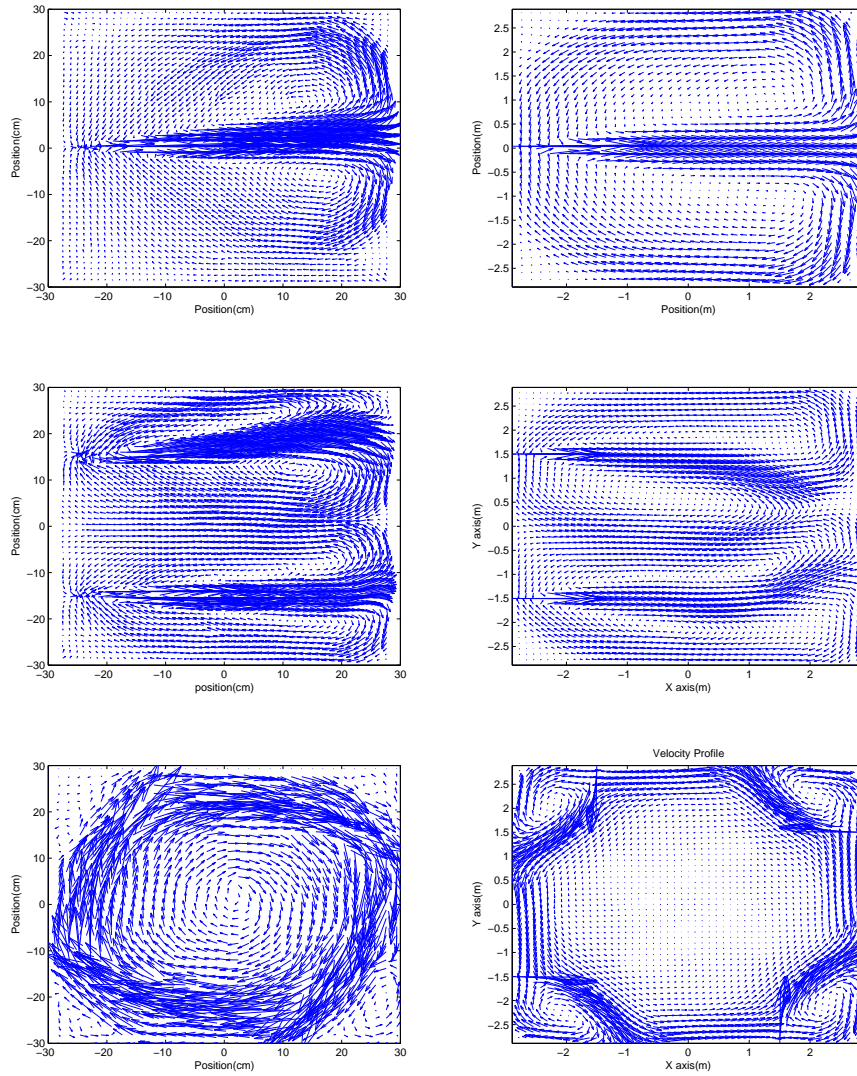


Figure 5: Horizontal velocity profile – experimental measurement (left column) and numerical simulation(right column): First row : One-source configuration, Second row : Two source with same direction($d/L=0.5$), Third row : Four-source configuration($R/L_2=0.5$)

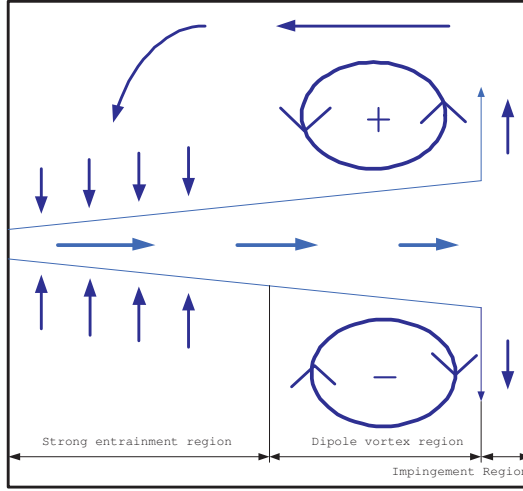


Figure 6: Schematic diagram of horizontal flow of the one-source configuration.

behavior (Fig. 8) A strong merged vortex in the middle still occurs but has two large counter vortices.

For the four-source jet configuration the positions of jets generate the initial angular momentum (Fig. 9). The integral of vorticity over the horizontal plane is zero and this circulation balance explains the dominant flow patterns for this configuration. The counter vortices are a result of this circulation balance and the Coanda effect which attracts jet onto the nearest wall. The circulation balance keeps the central vortex from growing and occupying the entire flow field and $R/\frac{L}{2}$ is the important factor in determining the size of the central vortex.

3.2 Thermal simulation of the plenum on each configuration

In order to estimate the thermal performance of the plenum, numerical simulations were carried out in which the lower boundary of the plenum is heated by the heat flux. This represents the heat transfer between floors in a multi-story building. The air flow rate from the inlets is $0.0043\text{m}^2/\text{s}$ at 288 K and the walls, excluding the bottom of the plenum, are assumed to be adiabatic. The base heat flux is 0.0614wm^{-2} , which makes the average temperature of the outlets increase by 4 K.

The calculated temperature contours at mid-depth of the plenum for each inlet configurations are shown in Fig. 10. Each configuration shows different horizontal temperature distributions, as a result of the different flow patterns. For the one-source configuration,

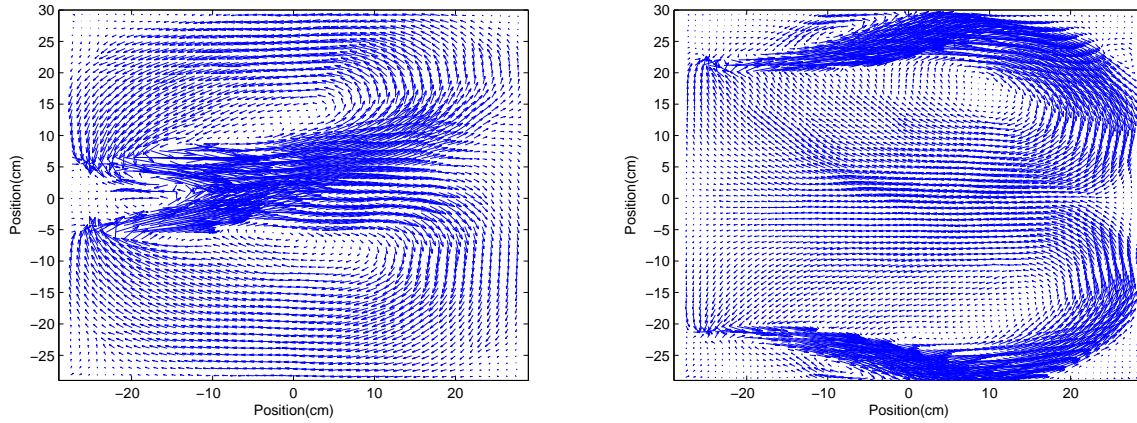


Figure 7: Horizontal velocity profile of experimental measurement of two sources with same direction: left figure: $d/L=0.2$, right figure: $d/L=0.7$

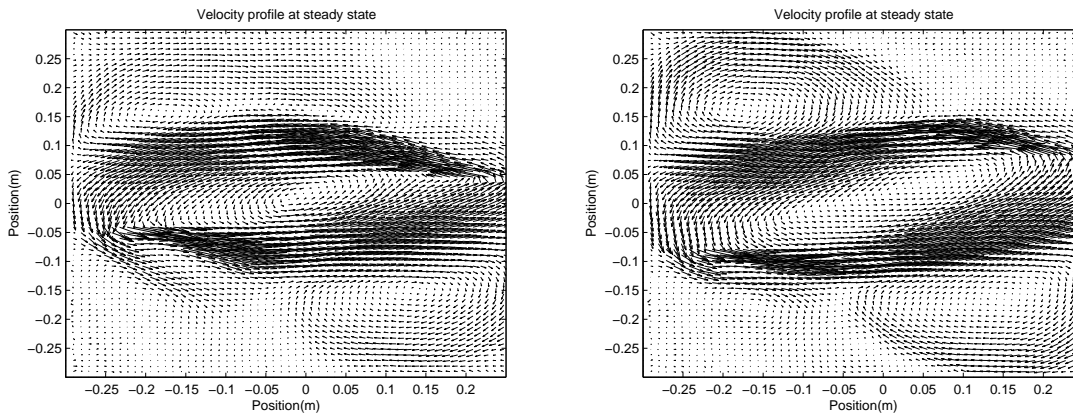


Figure 8: Horizontal velocity profile of experimental measurement of two sources with opposite direction: left figure: $d/L=0.133$, right figure: $d/L=0.267$

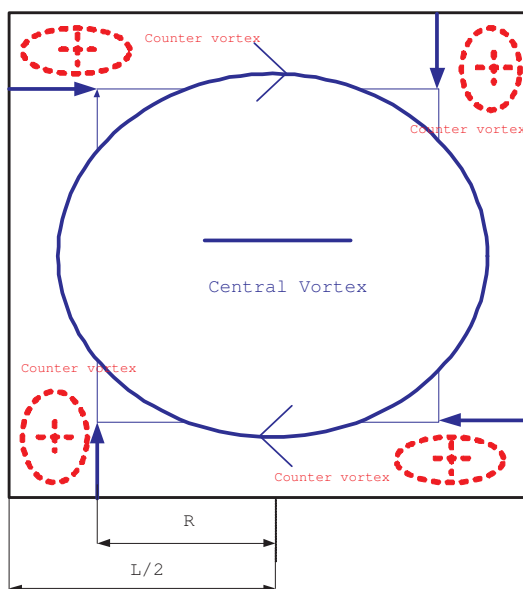


Figure 9: Schematic diagram of horizontal flow of four source jets.

the lower temperature region is found along the jet axis, however, the inner region of the dipole vortex has a relatively higher temperature by approximately 4 K. For the two-source configuration, the inner region of the dipole vortex has higher temperature similar to the one-source configuration.

The two-source and four-source configurations show relatively high temperatures in the center region which is dominated by the central vortex driven by the geometrical torque. The outer rim by the side wall maintains lower temperature because the paths of the inlet jets are steered toward the wall and they cool the region.

4 Discussion

4.1 Flow characteristic of each source jet configuration

The flow exhibits two-dimensional dynamics resulting from the shallow aspect ratio of the plenum. This, in turn, directly affects the flow patterns caused by the different arrangements of source configurations. This nature is apparent in the comparison of the numerics and experiments shown in fig. 11. The log-log graph of normalized centerline velocity and longitudinal distance has $-1/2$ slope, in agreement with plane jet theory. However, there is

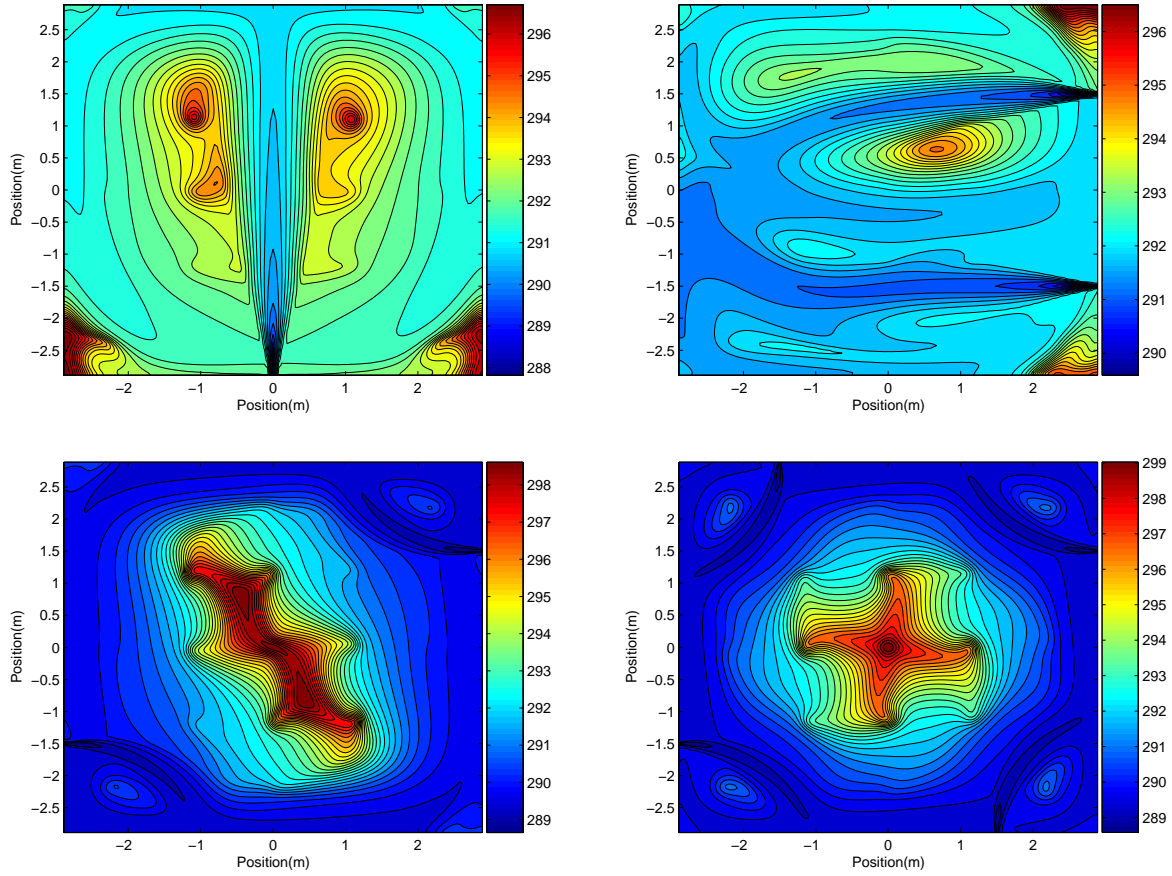


Figure 10: Temperature contour of each configurations at mid-depth: one source jet, two source jets with same direction, and two source jets with opposite direction, and four source jets.

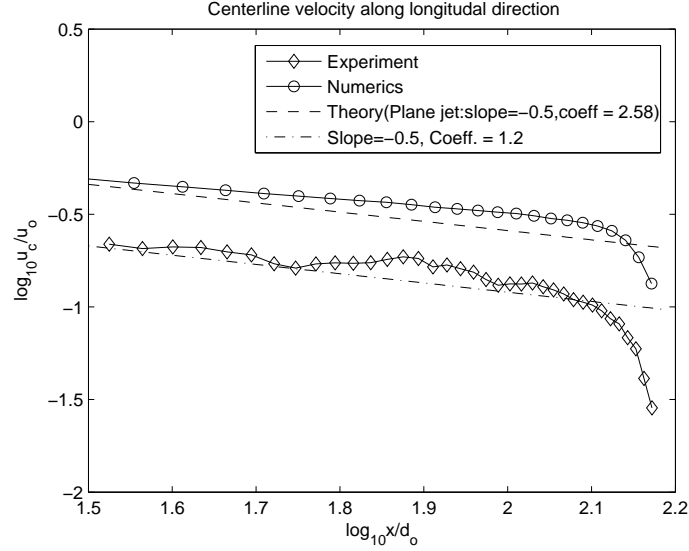


Figure 11: Log-Log graph of centerline velocity for experiment and numerical simulation.

mismatch of width of the jet between experiment and numerical simulation in Fig. 12. From plane jet theory, the jet width b has linear relation to the distance x given by $b = 0.12x$.

For the two-source configuration with same direction, the jets merge at a distance of 4.5 times the initial separation (Kaye & Linden 2004). However, in the present experiment the merging occurs much sooner at 1.4 times the initial separation. We suspect that the strong recirculation flow and the dipole vortex induced by merged jets in fig.7 can explain the strong attraction of two source jets.

For the four-source jet, the effective radius, $\sqrt{A/\pi}$ (A is the area of central vortex) and circulation vary according to the radius of the source position (Fig. 14). Interestingly, the effective radius is larger than the radius of source positions. That is because the strong recirculation vortex between source and nearest side wall produce a low pressure region and the source jet is steered toward the wall and generates a larger scale central vortex. However, the radius has linear relation to circulation, $\int \omega dA$, which is equal to the strength of the vortex-tube formed by all vortex lines passing through the edge of central vortex (Batchelor 1967).

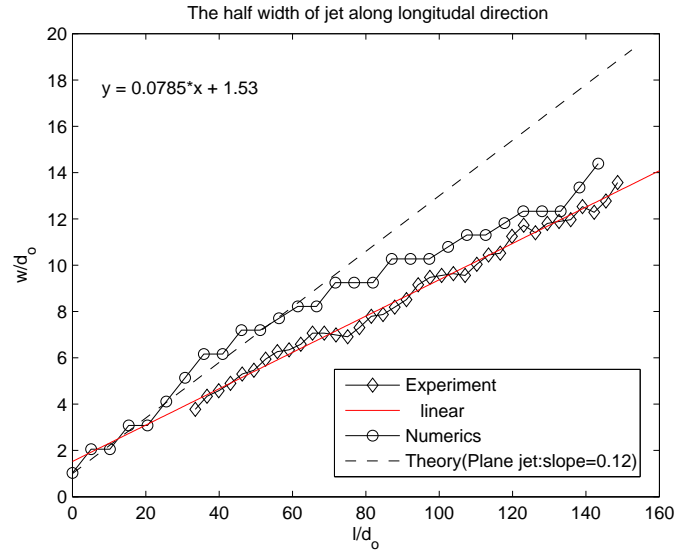


Figure 12: The width of jet propagation for experiment and numerical simulation.

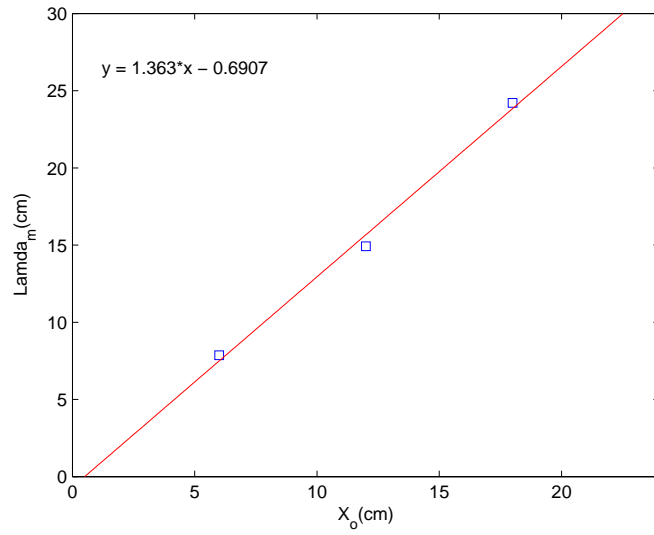


Figure 13: Jet merging height for equal jets plotted against initial separation.

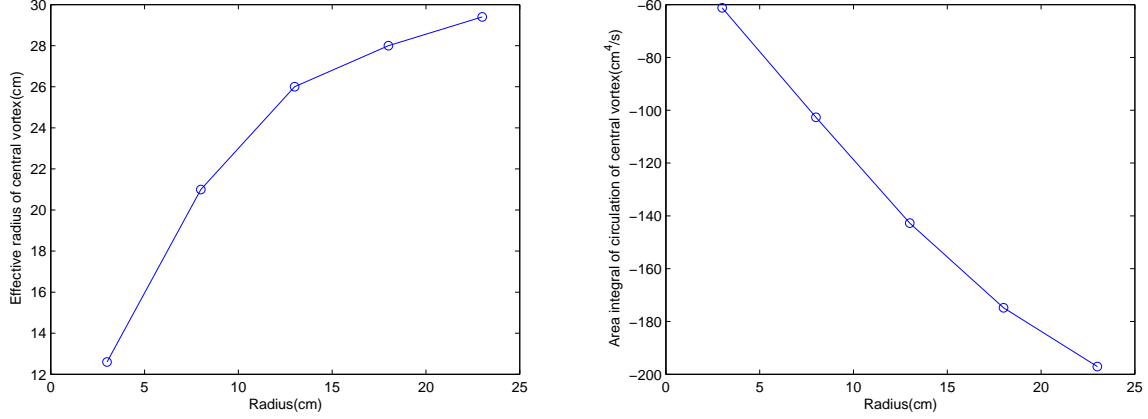


Figure 14: Radius *vs* effective radius of central vortex and radius *vs* circulation of central vortex in experiment.

4.2 Thermal characteristics of the plenum

The outlet temperature distribution of each configuration was calculated at $d/L = 0.5$ for the two-source configuration and $R/\frac{L}{2} = 0.5$ for the four-source configuration. The distribution of outlet temperature is closely related to temperature distribution of the mid-depth plane seen in fig.10. The cumulative histogram (fig. 15) shows that the one-source configuration has the narrowest band of temperature distribution as a result of the small dipole vortex region compared to large main stream and recirculating region.

In other multi-jet configurations, wider bands of outlet temperature distribution, which is undesirable for thermal comforts of occupants, were seen. However, the multi-jet configurations had more outlets below 292 K, which increases cooling efficiency locally (Fig. 16 and 17).

5 Conclusion

The flow patterns and the thermal characteristics of plenum flow in a UFAD system were studied using laboratory and numerical simulations for different numbers and geometrical arrangements of supply outlets. It was found that the flow was sensitive to the geometry of the forcing and that the thermal efficiency can be estimated by a cumulative histogram of temperature distributions. The four-source configuration, which generates initial torque, developed a large scale central vortex and provides flexibility of controlling the size of vortex.

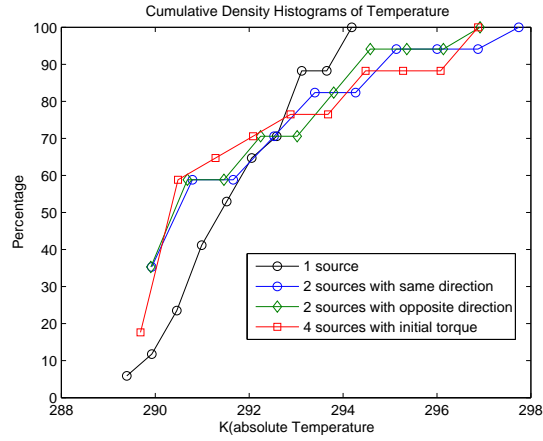


Figure 15: Cumulative histogram of all configurations.

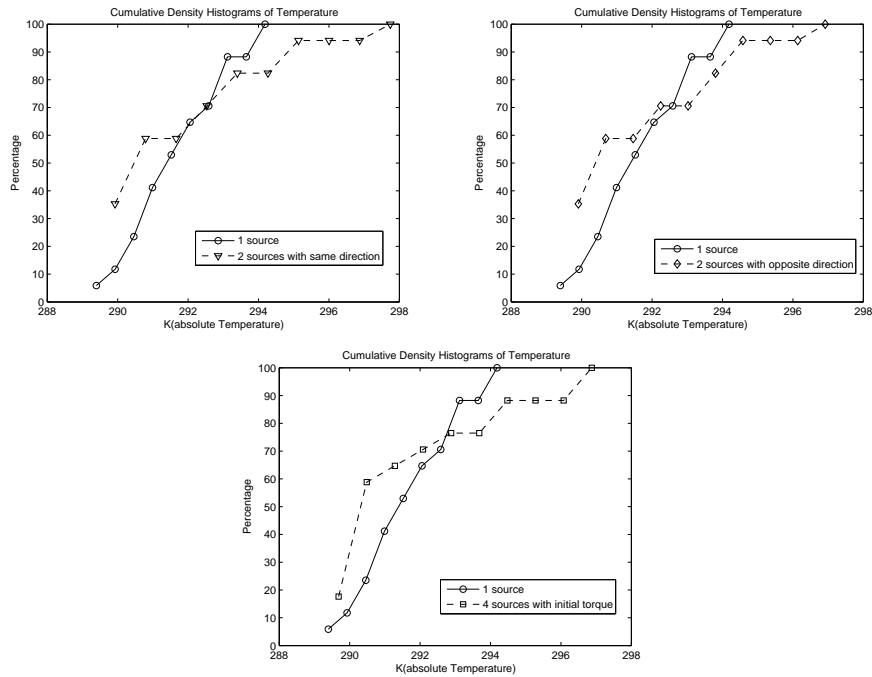


Figure 16: Cumulative histograms of one-source and two-source configurations with same direction, one-source and two-source configurations with opposite directions and the four-source configuration, respectively.

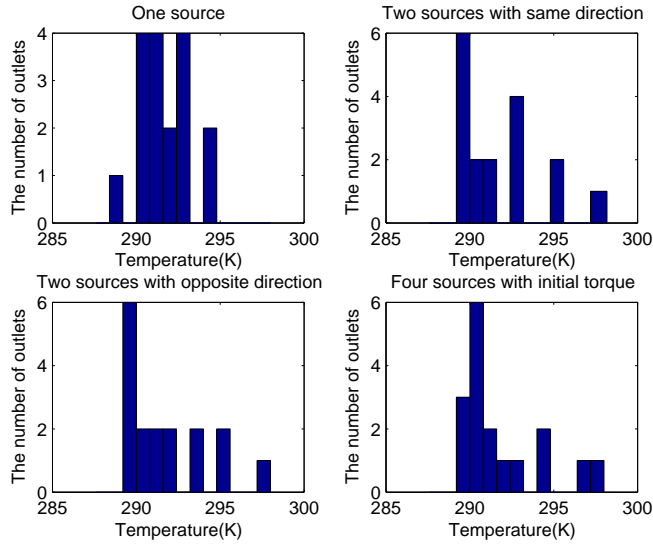


Figure 17: Histograms of all configurations.

Numerical simulation of the thermal characteristics of the supply plenum for each configuration shows that flow patterns are directly related to the outlet temperature distribution confirming the speculation that the different resident time is the cause of temperature variations in the plenum. The one-source jet configuration provides a good distribution of outlet temperatures and the multi-source configuration had a higher number of lower temperature outlets. This allows the multi-source to handle a larger cooling load.

References

- [1] Bauman, F. 2003. *Underfloor Air Distribution (UFAD) Design Guide*. Atlanta: ASHRAE, American Society of Heating, Refrigerating, and Air-Conditioning Engineers.,
- [2] Kanda, I. & Linden, P.F. 2001 Sensitivity of horizontal flows to forcing geometry. *J. Fluid Mech.*, **432**, 1–23.
- [3] Saffman P.G. 1992 Vortex dynamics *Cambridge university press*.

- [4] Kaye N.B. & Linden P.F. 2004 Coalescing axisymmetric turbulent plumes. *J. Fluid Mech.*, **502**, 41–63.
- [5] Choudhury D. 1993 Introduction to the Renormalization Group Method and Turbulence Modeling. *Fluent Inc. Technical Memorandum TM-107*
- [6] Bauman F., Hui Jin & Tom Webster Heat transfer pathways in Underfloor Air Distribution(UFAD)systems *ASHRAE Trans.*, *112(2)*, 2006
- [7] Lee J.H.W. & Chu V.H. Turbulent jets and plumes; A lagrangian approach *Kluwer Academic Publishers 2003*
- [8] Batchelor G.K. 1967 An introduction to fluid dynamics Cambridge university press